

A number of lines, usually parallel, is set out, and arrival times from each shot are recorded on all detectors. Shots are located so that a standard, in-line profile interpretation can be carried out on each line. This allows computation of time-depths at each detector position. These time-depths are then subtracted from arrival times for all shots, including shots sited on other lines, to produce travel times from each shot to a point on the refractor below each detector. The corrected arrival times for each shot are plotted on a plan of the survey lines and then contoured to produce wavefronts in the refractor.

The seismic velocity is obtained from the distance along the normal between the wavefronts, divided by the time increment (Palmer, 1986, chapter 2).

Data from localities at Foybrook and Mt. Bulga will demonstrate the method, its potential and its problems.

## References

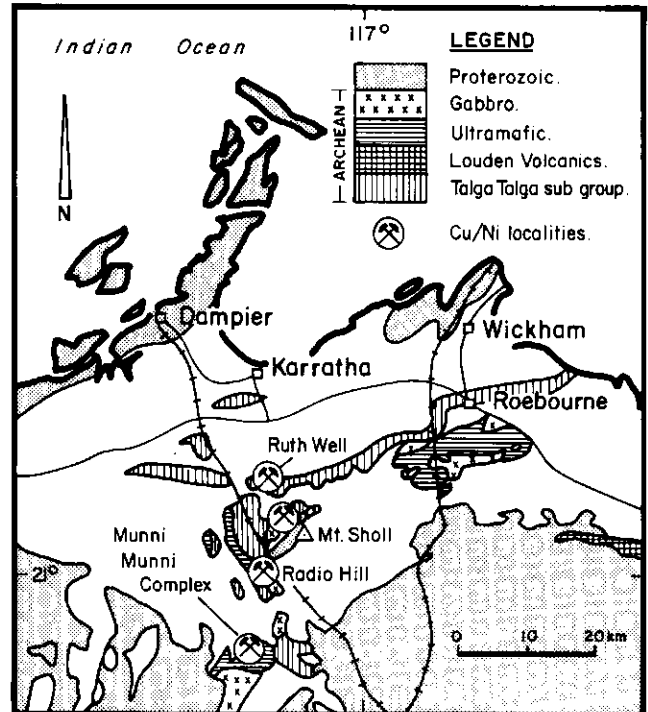
- Bamford, D. & Nunn, K. R. (1979), 'In-situ seismic measurements of crack anisotropy in the Carboniferous limestone of Northwest England', *Geophysical Prospecting* **27**, 322-338.
- Crampin, S., McGonigle, R. & Bamford, D. (1980), 'Estimating crack parameters from observations of P-wave velocity anisotropy', *Geophysics* **45**, 345-360.
- Dix, C. H. (1956), 'Seismic prospecting for oil', Harper and Row, New York.
- Mason, I. M. (1981), 'Algebraic reconstruction of a two-dimensional velocity inhomogeneity in the High Hazles seam of Thoresby Colliery', *Geophysics* **46**, 298-308.
- McGee, J. E. & Palmer, R. L. (1967), 'Early refraction practices in seismic refraction prospecting', A. W. Musgrave, Ed, SEG, Tulsa, pp. 3-11.
- Nettleton, L. L. (1940), 'Geophysical prospecting oil', McGraw-Hill, New York.
- Palmer, D. (1986), 'Refraction seismics', Geophysical Press, Amsterdam.
- Sjogren, B. (1984), 'Shallow refraction seismics', Chapman and Hall, London.
- Worthington, M. H., Mason, I. M. & Wheller, P. M. (1983), 'Application of seismic tomography to mineral exploration', *Trans. Inst. Min. Metall.* **92**, B209-B213.

## THE RADIO HILL NI-CU MASSIVE SULPHIDE DEPOSIT A GEOPHYSICAL CASE HISTORY

W. S. Peters, M. de Angelis

### Introduction

The Radio Hill Ni-Cu deposit is situated approximately 30 km south of Karratha in Western Australia (Fig. 1). It was originally located by Westfield Minerals (WA) N.L. in 1972 as an aeromagnetic anomaly with coincident weak Ni-Cu soil geochemistry in an area of no outcrop. Between that time and 1978 various geophysical surveys and drilling failed to locate significant mineralisation. Between 1981 and 1986 geophysical surveys and drilling by Teck Explorations Limited



REGIONAL GEOLOGY & LOCATION MAP

FIGURE 1

Regional geology and location map.

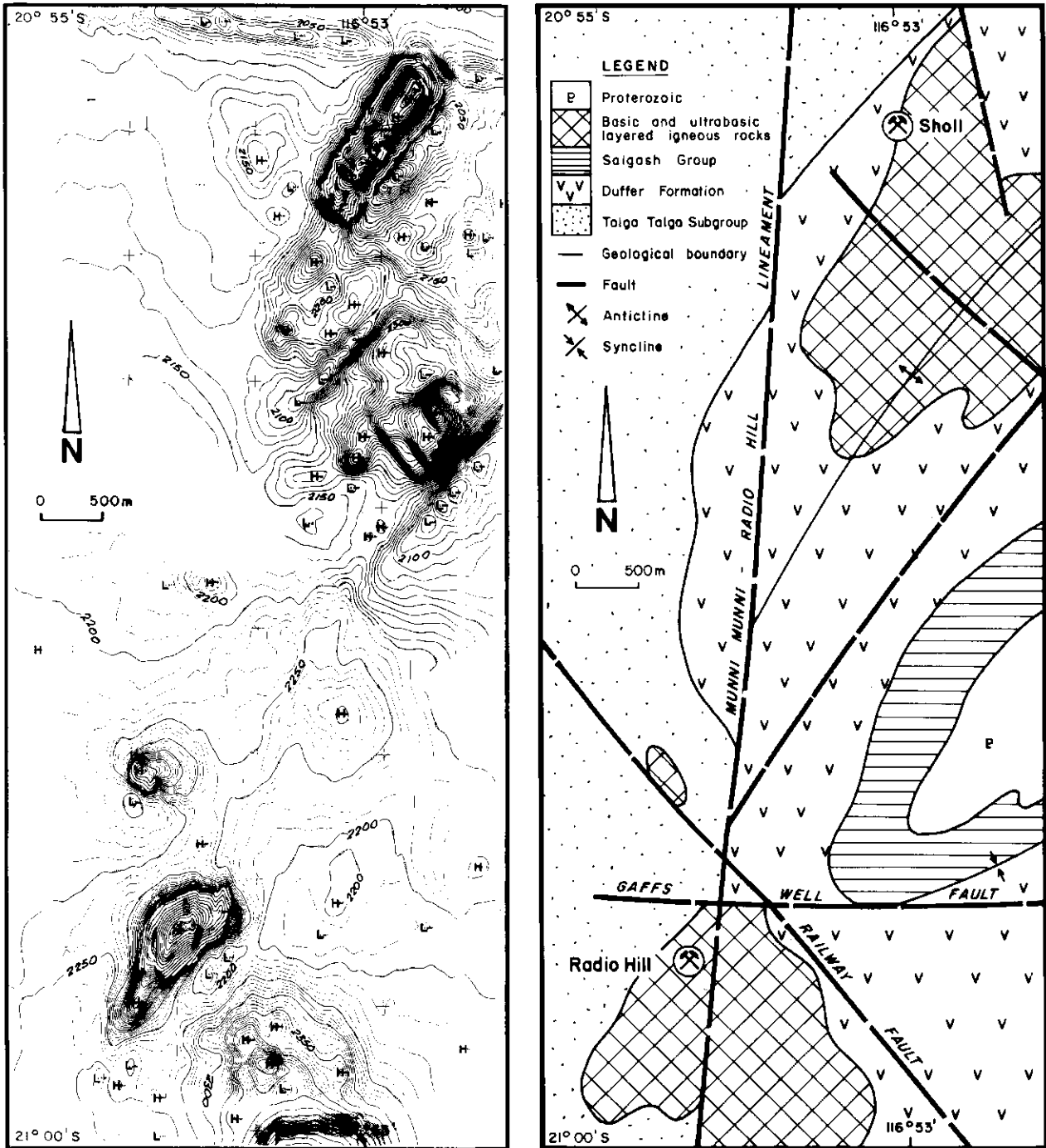
and Samim Australia Pty Ltd located a significant Ni-Cu sulphide deposit. Table 1 summarises the geophysical surveys carried out over the area.

TABLE 1  
Geophysical survey summary

METHOD	YEAR	COMMENTS
Aeromagnetic	1968	U.S. Steel : 400m Line spacing
Ground Magnetic	1972	Whim Creek - Westfield Minerals : 120m x 30m Grid.
Turam	1972	" " " " : 120m x 30m Grid.
Crane P.E.M.	1978	" " " " : Two Lines only
Aeromagnetic	1981	Teck Explorations : 50m Line Spacing.
Siratem	1982	" " " " : Offset 100m Loops, 100m x 50m Grid.
Ground Magnetic	1984	Samim Australia : 50m x 10m Grid.
Applied Potential	1984	" " " " : 50m x 25m Grid.
EM 37	1984	" " " " : 50m x 50m Grid
Downhole Siratem	1985	" " " " : 12 Holes, 7 TX Loops
Gravity	1986	" " " " : Two Lines only.

### Geology

The deposit is hosted within one of several layered mafic/ultramafic intrusions emplaced in the Archaean sequence of the western Pilbara Block (Figs 1, 2). The sequence has been invaded regionally by granite gneiss and intruded by granite plugs, the layered mafic/ultramafic bodies, and basic igneous rocks. Proterozoic basalts overlie the sequence and the area is extensively intruded by younger dolerite sills and dykes (Cooya Pocyia Dolerite). Several major lineaments and faults have been identified from Landsat and aeromagnetics.



**FIGURE 2**  
Regional aeromagnetics and geology.

There is no outcrop in the mineralised area at Radio Hill. Drilling information shows that the layered intrusion dips shallowly to the southeast and consists of a basal ultrabasic/basic sequence overlain by a layered metagabbro sequence. A later steeply dipping feldspathic gabbro dyke cuts the sequence and forms the Radio Hill topographic feature. The entire complex is bounded east and west by basement metabasalts and to the south by granite.

The mineralisation is blind and lies beneath overlapping basement volcanics at its shallowest point (17 m). It is present

in disseminated form (primary) in peridotite/dunite units and in stringer/massive form (remobilised) in gabbro/pyroxenite units at the basement contact. The soil Ni-Cu geochemical anomaly is reflecting the peridotite/dunite units. The sulphides are mainly pyrrhotite, chalcopyrite and pentlandite. Magnetite is present and also tellurides of Pd, Bi and Pb. Trace elements include Co, Au, Zn and Sn.

The geological resource amounts to 2.5 Mt of 1.5% Ni and 1.4% Cu using 0.8% Ni + Cu and 2 m true thickness cut-offs. This includes a higher grade zone of 0.57 Mt of 2.5%

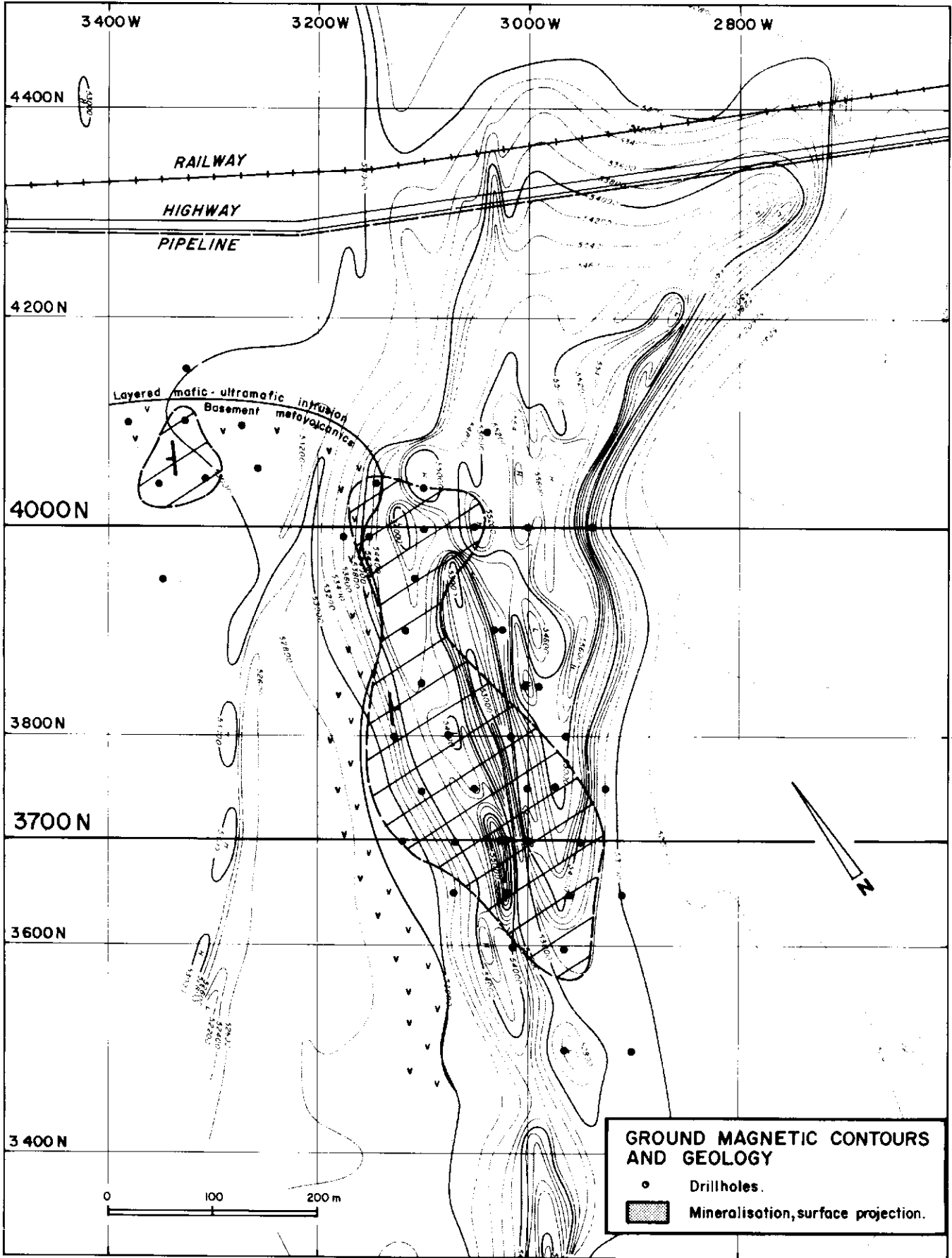


FIGURE 3  
Ground magnetics and geology.

Ni and 2.3% Cu using 2% Ni + Cu and 2 m true thickness cut-offs.

**Aeromagnetic Surveys**

The first aeromagnetic survey over the area was flown by US Steel in 1968 using 400 m line spacing. This survey was used in the 1970s to locate the layered mafic/ultramafic intrusions prior to ground work. A very detailed survey using 50 m line spacing (Fig. 2) was flown in 1981 and showed that the Radio Hill area had a discrete magnetic anomaly of about 750 nT which was similar in character to the anomaly over the Sholl mineralised intrusion to the north.

**Ground Magnetic Surveys**

A ground magnetic survey carried out in 1972 using a 30 m x 120 m grid was used largely to locate the target area. A more detailed survey was carried out in 1984 using a 10 m x 50 m grid (Figs 3, 6). This showed shallow multiple northeast striking magnetic units and transgressive dykes and faults. Interpreted dips were steeply southeast. Susceptibility logging of core has revealed that the magnetic anomalies are largely due to peridotite units overlying the sulphide mineralisation. The massive sulphide zone contains predominately non-magnetic hexagonal pyrrhotite and does not cause a significant magnetic response at surface.

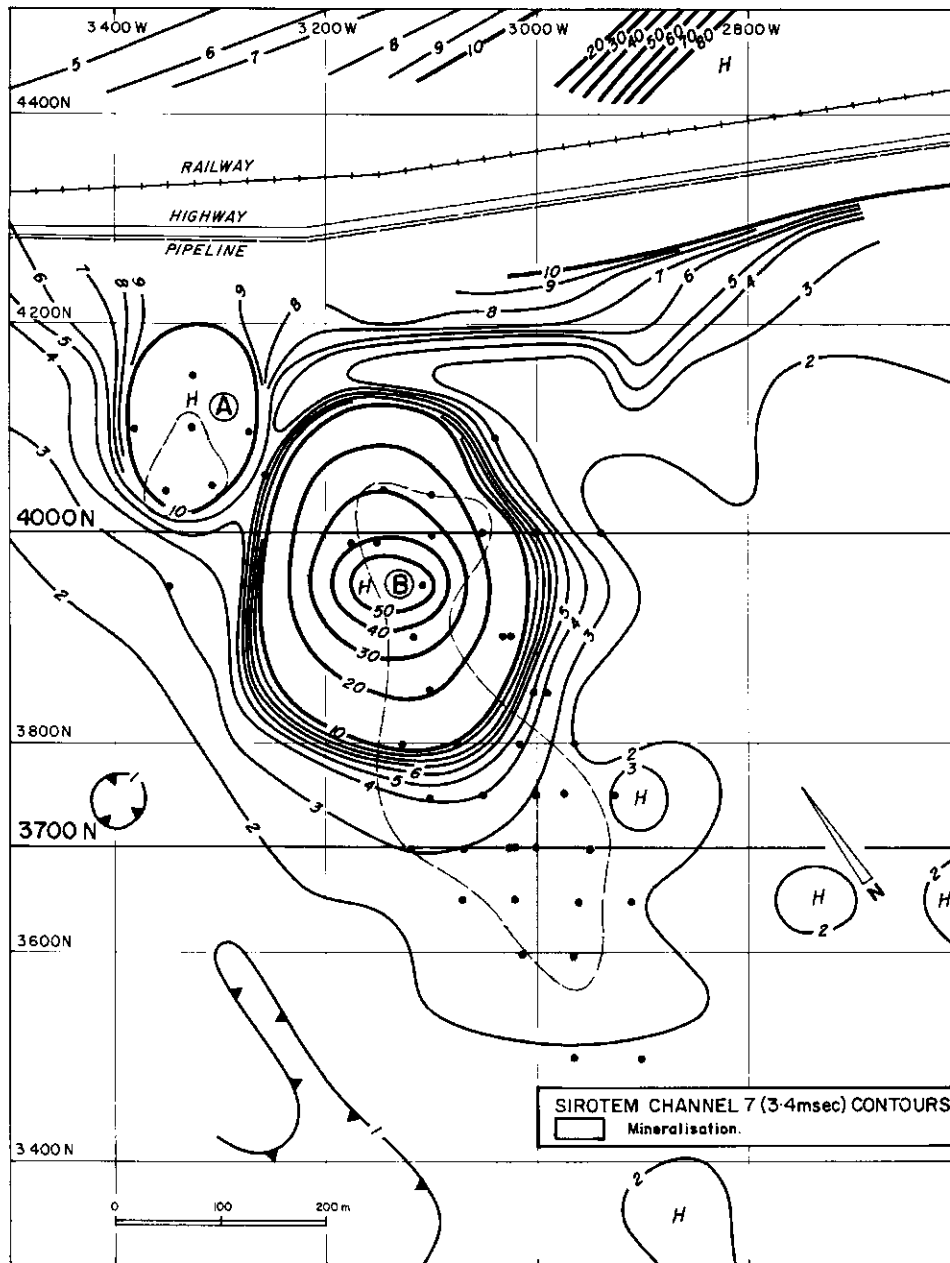


**FIGURE 4**  
SIROTEM Channel 7 (3.4 m/s) contours.

## TURAM and CRONE PEM Surveys

Profiles from these surveys are shown in Fig. 6. The TURAM survey was carried out in 1972. It was not very effective but Hole 2 sited on a weak quadrature anomaly on line 4000 N intersected minor mineralisation. In 1978 a Crone PEM survey over line 4000 N detected an excellent conductor. Earlier percussion holes on a geochemical anomaly in this area were unsuccessful, having stopped short of the conductor and it was not tested further.

## Surface SIROTEM Survey

In 1982 a SIROTEM survey using 100 m offset loops was carried out over the area. The channel 7 (3.4 m/sec) voltage

contours (Fig. 4) delineated the two excellent conductors A and B in addition to high responses from the railway and pipeline cutting the area. Conductor B was interpreted to plunge to the south. The profiles for a shallow part (3950 N) and a deeper part (3750 N) of conductor B are shown in Figure 6. The early time negative feature east of the main anomaly is thought to be a current channeling effect. Time constants range from 5 m/sec to 12 m/sec. Drilling of the highest amplitude parts of the two anomalies resulted in marginal intersections of up to 24 m of 0.86% Ni + Cu.

## Applied Potential Survey

In 1984 an applied potential survey was carried out using downhole current electrodes placed in the mineralisation

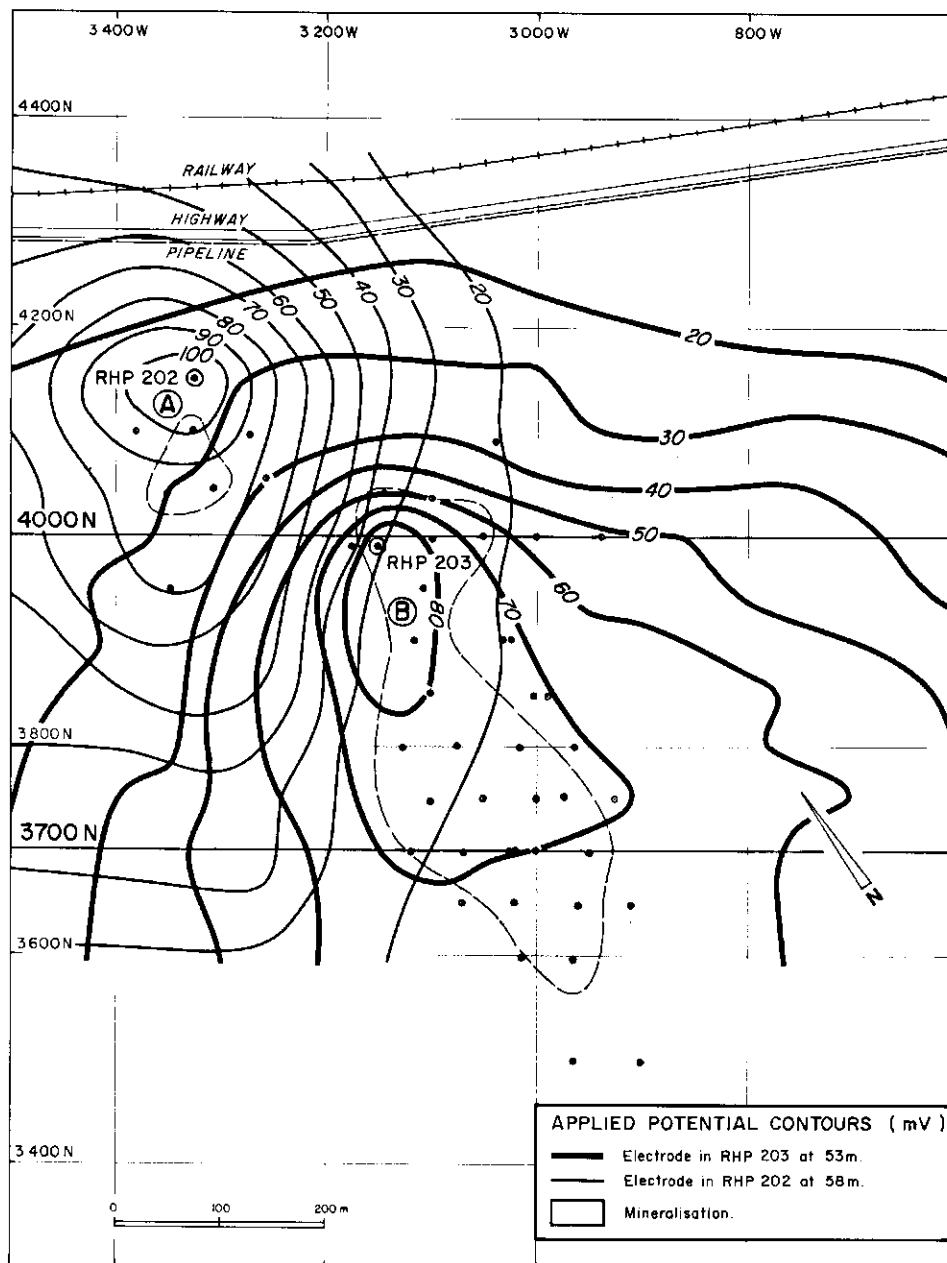


FIGURE 5  
Applied potential contours.

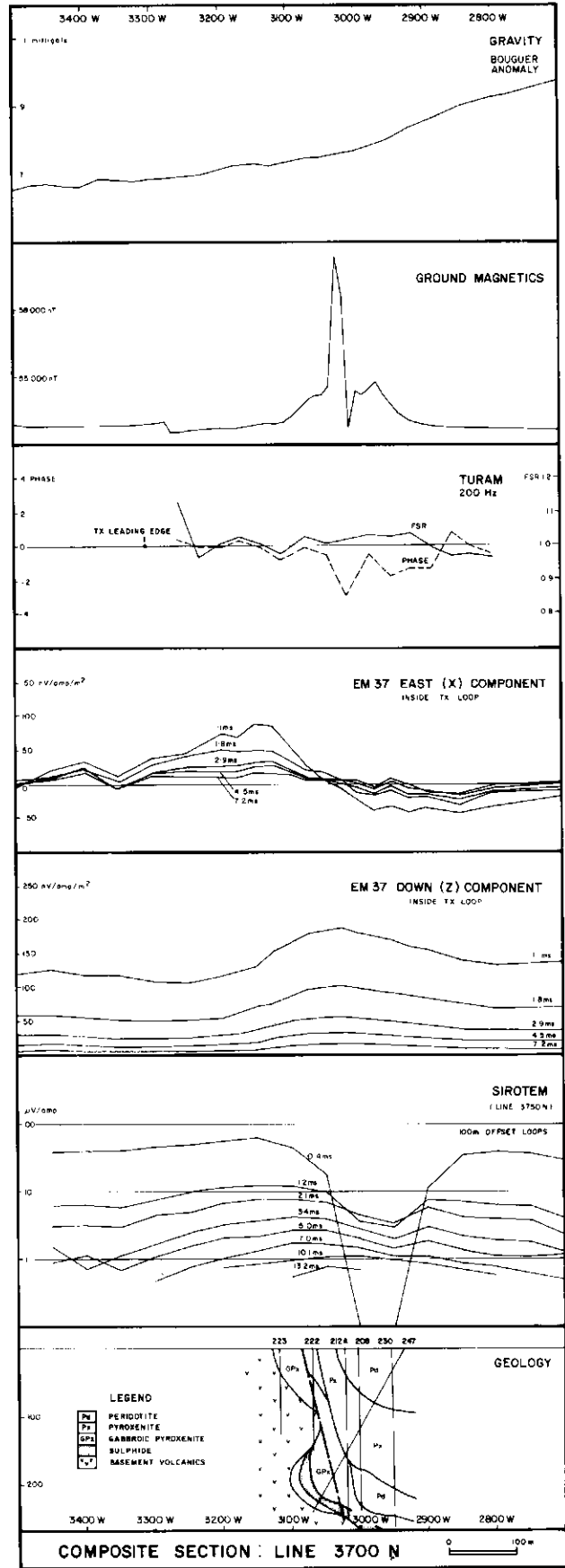
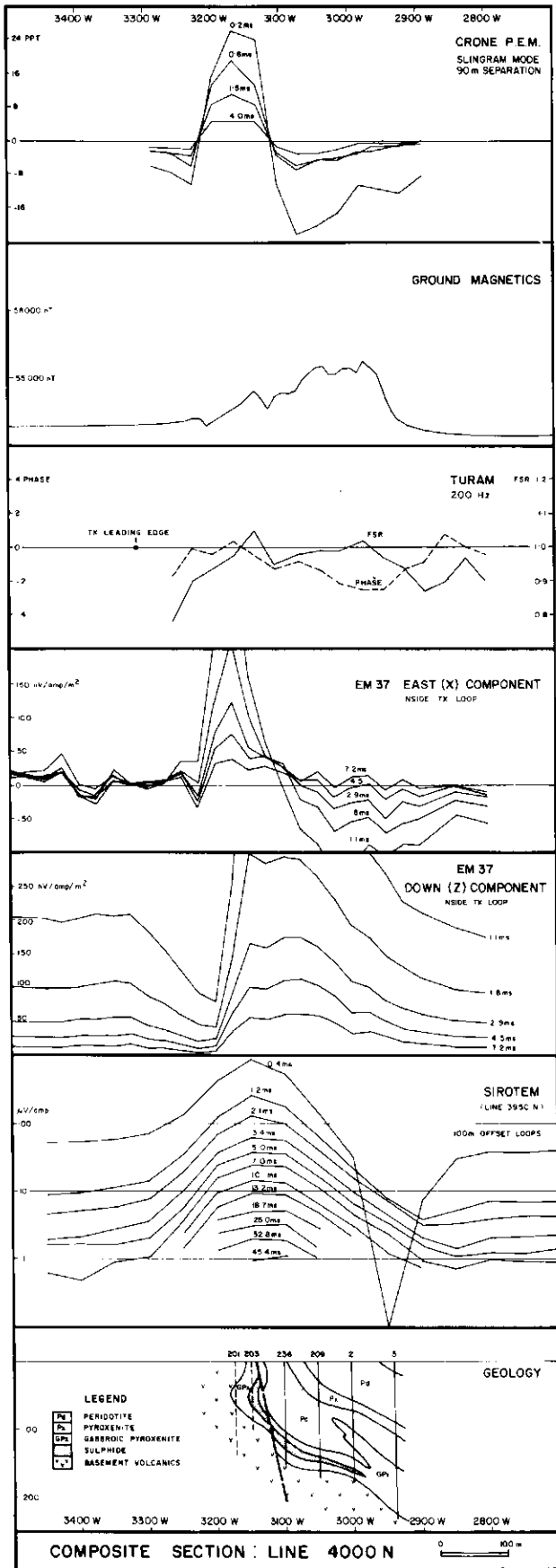


FIGURE 6  
Composite geophysical profiles and geological sections for 3700 N and 4000 N.

intersected on conductors A and B. The potential contours using two different electrodes are shown in Fig. 5. The data was interpreted as reflecting two separated bodies both plunging to the south with conductor A west and conductor B dipping east. Drilling on conductor B resulted in the "discovery" hole with 18 m of 3.95% Ni + Cu at 160 m.

### EM37 Fixed Transmitter Loop Survey

This survey was carried out in 1984 within large (800 m × 600 m) transmitter loops placed over the mineralisation. Profiles of the down (Z) and east (X) components are shown in Fig. 6. This delineated an interpreted plate-like body with strike length of 600 m dipping about 35 degrees east and plunging 20 degrees south with a depth ranging from 70 m in the north to 300 m in the south. The subsequent drilling that outlined the deposit was based upon this model which proved substantially accurate.

### Downhole SIROTEM Survey

Downhole SIROTEM surveying was carried out in 1985 but this was severely hampered by blocked holes. The data collected in the few holes successfully logged showed good responses and the method would be a considerable aid in exploration of similar deposits if holes were preserved.

### Gravity Survey

A gravity survey on line 3700 N (Fig. 6) failed to detect the mineralisation or outline any useful structure.

### Conclusions

The Radio Hill discovery is an example of using regional geophysical methods to firstly locate a target area based on a conceptual model and then detailed ground geophysics to ultimately delineate a blind massive sulphide resource. It has demonstrated the value of the vastly improved electromagnetic systems now available and shown that considerable persistence on a target can be worthwhile.

### Acknowledgements

We wish to thank Samim Australia Pty Ltd, Teck Explorations Ltd and Whim Creek Consolidated N.L. for permission to publish this paper.

## THE USE OF 'AUTOMATIC GAIN CONTROL' TO DISPLAY VERTICAL MAGNETIC GRADIENT DATA

Shanti Rajagopalan

### Introduction

Magnetic anomalies vary widely both in amplitude and in spatial frequency. As conventional methods of presenting total field data tend to highlight regional anomalies, vertical gradient (VG) data is often used to delineate high-frequency anomalies. While collecting gradient data as part of an aeromagnetic survey is becoming more common, it is also possible to approximate it by using high-pass filters or Fourier Transforms. However, presenting gradient data is more of a problem than computing it. Contour maps are difficult and expensive to produce. Significant, low-amplitude anomalies may not be clearly represented. In addition, the large number of closures characteristic of a VG contour map can make the choice of contour levels and the identification of trends difficult.

Stacking profiles would remove the disadvantages inherent in contouring (McIntyre 1981). To be able to use stacked profiles like a map and compare it with other maps, the anomalies must be plotted at or close to their true locations, and at a vertical scale that would aid trend analysis. The first is easily achieved by making the baseline or background level of each profile coincide with the flight path. It is generally not possible to achieve the second using a linear vertical scale as a small scale might obscure fine detail while a larger scale could lead to overprinting of profiles and reduced clarity. A non-linear scale would overcome this problem. It is suggested here that the method of 'Automatic Gain Control' (AGC), used in electronic systems and in displaying seismic data, can be successfully used to display gradient data.

### Automatic Gain Control

Almost all home radios use AGC to compensate for amplitude variations in the carrier wave signal. In the ideal AGC amplifier, shown in Fig. 1, the gain of the amplifier varies with the amplitude of the input signal in such a way that the output amplitude is kept constant (Schilling 1968).

By simulating the electronic amplifier digitally, AGC can be applied to discrete VG data. Within a window sliding along the profile, the root mean square (RMS) value is computed.

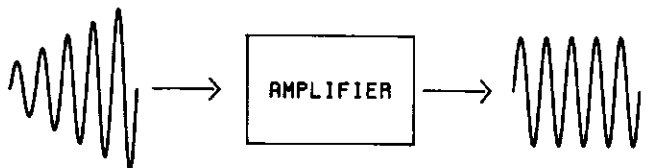


FIGURE 1  
Action of the ideal AGC amplifier.